Electrical-Driven Transport of Endohedral Fullerene Encapsulating a Single Water Molecule

Baoxing Xu[1] and Xi Chen[1,2,3,*]

[1]Department of Earth and Environmental Engineering, Columbia Nanomechanics Research Center, Columbia University, New York, New York 10027, USA

[2]SV Lab, International Center for Applied Mechanics, School of Aerospace, Xi'an Jiaotong University, Xi'an 710049, China

[3]Department of Civil and Environmental Engineering, Hanyang University, Seoul 133-791, Korea

(Received 14 September 2012; revised manuscript received 2 February 2013; published 12 April 2013)

Encapsulating a single water molecule inside an endohedral fullerene provides an opportunity for manipulating the $H_2O@C_{60}$ through the encapsulated polar H_2O molecule. Using molecular dynamic simulations, we propose a strategy of electrical-driven transport of $H_2O@C_{60}$ inside a channel, underpinned by the unique behavior of a water molecule free from a hydrogen-bonding environment. When an external electrical field is applied along the channel's axial direction, steady-state transport of $H_2O@C_{60}$ can be reached. The transport direction and rate depend on the applied electrical intensity as well as the polar orientation of the encapsulated H_2O molecule.

DOI: 10.1103/PhysRevLett.110.156103 PACS numbers: 68.08.−p, 62.23.−c

Trapping a single atom or molecule inside the hollow interior of a fullerene such as C_{60} has drawn significant attention because of its unique closed-cage structure and unconventional property [1–5]. The synthesized endohedral fullerene provides a rich and fascinating platform inside which a single atom or molecule may be placed, and the isolated status of the molecule and its "communication" with the surrounding environment may lead to interesting characteristics and novel functionalities [6,7]. For example, the pure C_{60} itself does not have a dipole, whereas $H_2O@C_{60}$ is a polar molecule due to the high dipole moment of the encapsulated H_2O molecule [8]. The introduction of a dipole moment provides a possibility for manipulating C_{60} through the encapsulated H_2O molecule. On the other hand, many fascinating properties of nanoconfined water, such as an unusual phase transition [9,10] and enhanced transport rate [11–14], are dominated by the pervasive hydrogen bonds. Thus, the possibility of isolating a single molecule of H_2O into the C_{60} cage opens a door to reveal the intrinsic properties of the single water molecule free from any hydrogen-bonding environment. Using molecular dynamics (MD) simulations, we propose herein (for the first time to the best of our knowledge) a controllable transport mechanism of $H_2O@C_{60}$ in a channel, where the motion of the encapsulated H_2O molecule is driven by an external electrical field.

Since the encapsulated H_2O molecule does not affect the structure of the outer C_{60} cage (see Figs. S1a and S1b [15]), this is also consistent with results from *ab initio* MD by Bucher [16], and thus the C_{60} is assumed rigid here. The water molecule is modeled by the most popular extended simple point charge (SPC/E) potential [17]. The 12-6 pairwise L-J potential and Coulomb interaction are used to model the water-water interaction and carbon-water interaction (see the Supplemental Material [15] for the detailed force field and L-J parameters). A single water molecule is placed inside the C_{60}. After equilibrium at temperature of 300 K and 1 atm, the oxygen atom of the encapsulated H_2O molecule is located at the center of the C_{60} cage (see Fig. S1c [15]), consistent with the experimental observation [8]. A segment of smooth carbon nanotube (CNT), which has a linear structure and slippery surface [18], is employed as a channel inside which the $H_2O@C_{60}$ transports. The radius of the CNT (4.1 nm) is chosen to be large enough in comparison with the size of $H_2O@C_{60}$ (outer radius: 0.5 nm; inner radius: 0.175 nm) so as to minimize the effect of the CNT wall. The CNT channel is assumed rigid and kept fixed throughout simulation, and its length (19.5 nm) is confirmed to be long enough for robust numerical results. Periodical boundary condition is imposed in the axial direction of the computational cell so as to mimic an infinite long channel. The $H_2O@C_{60}$ is placed into the CNT channel and equilibrated for a period of time t_0 (see Fig. S2 [15]). An external electrical field E is then imposed in the axial direction of the CNT channel (i.e., $+z$ direction). We should note that the C_{60} cage behaves like a set of separate carbon atoms in a static electrical field and will not fully screen out the external electrical field [19]. Additional MD simulation [with the dielectric constant $\varepsilon(=4.5)$ [20], using LAMMPS with the NVT ensemble, at 300 K by using the Nose-Hoover thermostat [21]) and density functional theory calculations are carried out to confirm the relatively minor role of screening effect; see the Supplemental Material [15].

Regardless of the magnitude of the applied electrical intensity, the $H_2O@C_{60}$ always transport along the axis of the tube (see Supplemental Material movie MS1 [15]). For C_{60}, only the translation is observed and there is no rotational motion during transport; meanwhile, for the water molecule, the oxygen atom follows the transport trajectory, yet the H_2O molecule keeps rotating itself, which is analyzed below. Under a smaller electrical intensity,

e.g., $E = 0.02$ V/Å, the $H_2O@C_{60}$ transports along the opposite direction of the applied electrical direction (i.e., $-z$ direction), and the snapshots from MD simulations are given in Figs. 1(a) and 1(b) presents the transport history of $H_2O@C_{60}$ along the z direction and a constant axial transport rate is observed, which demonstrates that an external electrical field may drive the motion of $H_2O@C_{60}$ in a stable manner, similar to a nanofluidic electroactuation system [22]. When the screening effect of C_{60} is considered, the stable transport manner will not change (see Fig. S3 [15]), and this is also confirmed by density functional theory dynamic calculations (see Fig. S11 [15]). Note that at a larger electrical intensity, the steady transport direction may be aligned in the same direction with the electrical field (i.e., $+z$ direction), as shown in Fig. S4b and the movie MS2 [15] under $E = 0.1$ V/Å. In the current study, such an inversion of transport direction happens at 0.065 V/Å.

To reveal more transport details of $H_2O@C_{60}$, the polar orientation of the encapsulated H_2O molecule is investigated, whose instantaneous inclination angle θ_t [Fig. 2(a)] with regard to the electrical field direction (i.e., $+z$) is given in Fig. 2(a), with $\theta_t = \cos^{-1}(p_t \frac{\hat{\mu}}{|p_t|})$ [23]. Here, $\hat{\mu}$ is a unit vector along $+z$, t represents a time instant, and p_t is the instantaneous dipole of the H_2O molecule pointing from the H shell to the O shell. During equilibrium and before the electrical field is applied ($t \leq t_0$), θ_t fluctuates randomly [Fig. 2(b)]. After an electrical field is applied at t_0, θ_t quickly becomes stable—such a steady-state value of the inclination angle of polar orientation of H_2O is referred to as θ_{ts}. Figure 2(b) shows that in the case of $E = 0.02$ V/Å ($t_0 = 0.055$ ns), θ_{ts} keeps 68.9° after about $t = 0.1$ ns, consistent with the constant axial transport rate of $H_2O@C_{60}$ [Fig. 2(a)].

Because of the random rotation of an H_2O molecule during equilibrium, the inclination angle at the beginning instant of application of the electrical field $\theta_0 = \theta_{t=t_0}$ is also random. Nevertheless, Fig. 3(a) shows that the steady-state θ_{ts} is independent of θ_0. That is, after the electrical field is applied, the steady-state polar orientation "axis" of H_2O, θ_{ts}, depends only on the magnitude of E. Generally, a stronger electrical field tends to align the dipole closer to the direction of the electrical field, leading to a smaller θ_{ts} during transport, which is consistent with present simulation [see Fig. S5]. A series of simulations show that when θ_{ts} is beyond a critical value (i.e., if the electrical field is not strong enough), there is no stable axial transport of $H_2O@C_{60}$, referred to as an unstable state here. Based on the one-to-one correspondence between E and θ_{ts}, a map of the electrical field-driven transport status of $H_2O@C_{60}$ is plotted in Fig. 4, where the axial transport of $H_2O@C_{60}$ is along the $-z$ direction in region I ($26.7° < |\theta_{ts}| < 82.6°$ and 0.006 V/Å $< E < 0.065$ V/Å), along the $+z$ direction in region II ($0 \leq |\theta_{ts}| \leq 26.7°$ and $E \geq 0.065$ V/Å), and unstable in region III ($0 \leq E \leq 0.006$ V/Å) (i.e., flips randomly in the channel). During the stable translational

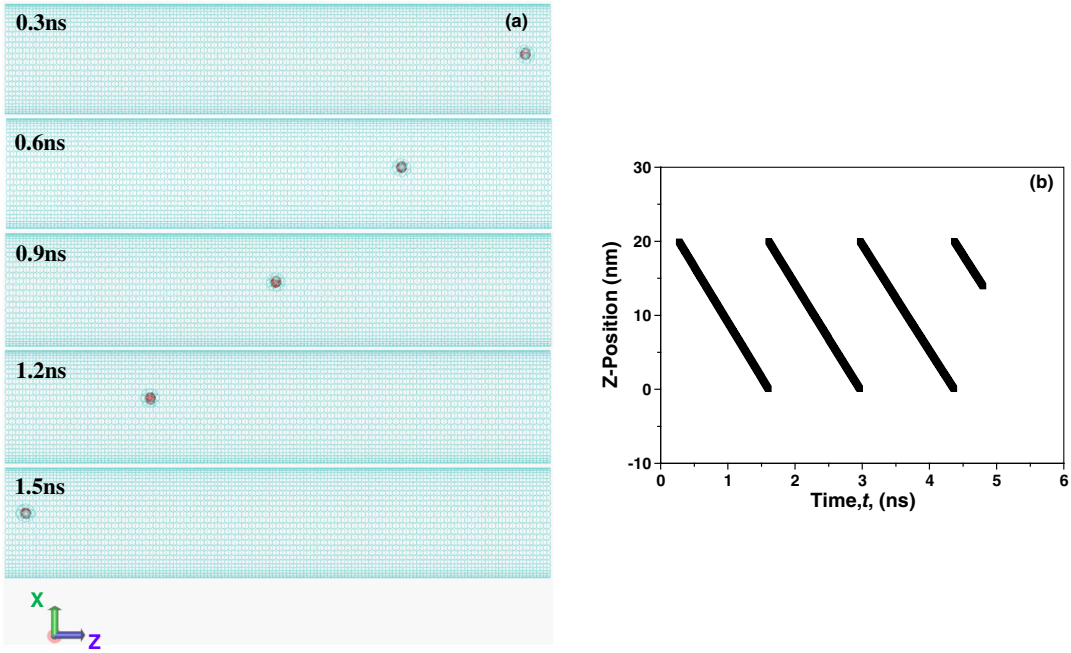

FIG. 1 (color online). An electrical field is applied along the $+z$ direction of a CNT channel, with electrical intensity $E = 0.02$ V/Å. (a) Snapshots of $H_2O@C_{60}$ transport along the $-z$ direction. (b) Axial position transport history of $H_2O@C_{60}$; note that a periodic boundary condition is applied in the axial direction, and thus the $H_2O@C_{60}$ transports along the $-z$ direction in an infinitely long channel at a steady rate.

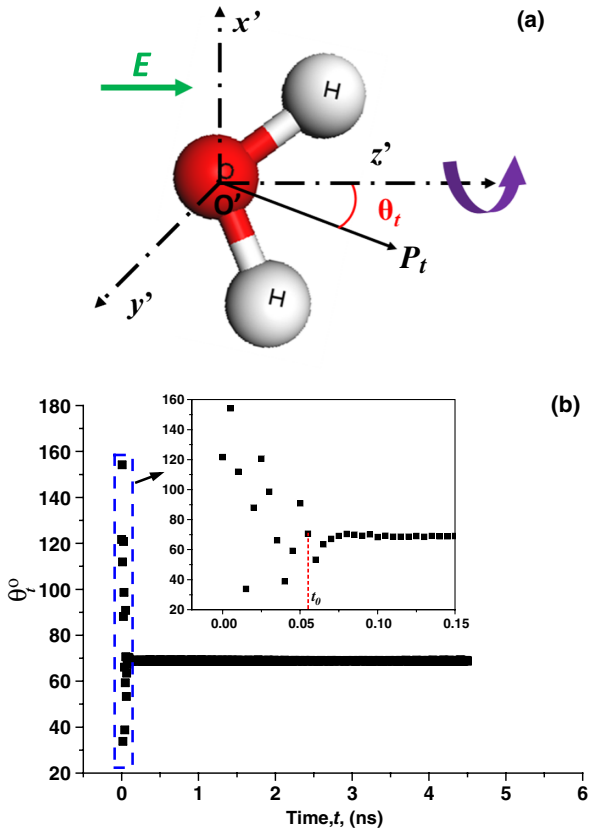

FIG. 2 (color online). (a) Schematic of the instantaneous inclined angle (θ_t) between the instantaneous dipolar orientation (p_t) of the encapsulated H_2O and unit vector ($\hat{\mu}$) along the electrical field direction. (b) The history of θ_t during the transport of $H_2O@C_{60}$ under $E = 0.02$ V/Å.

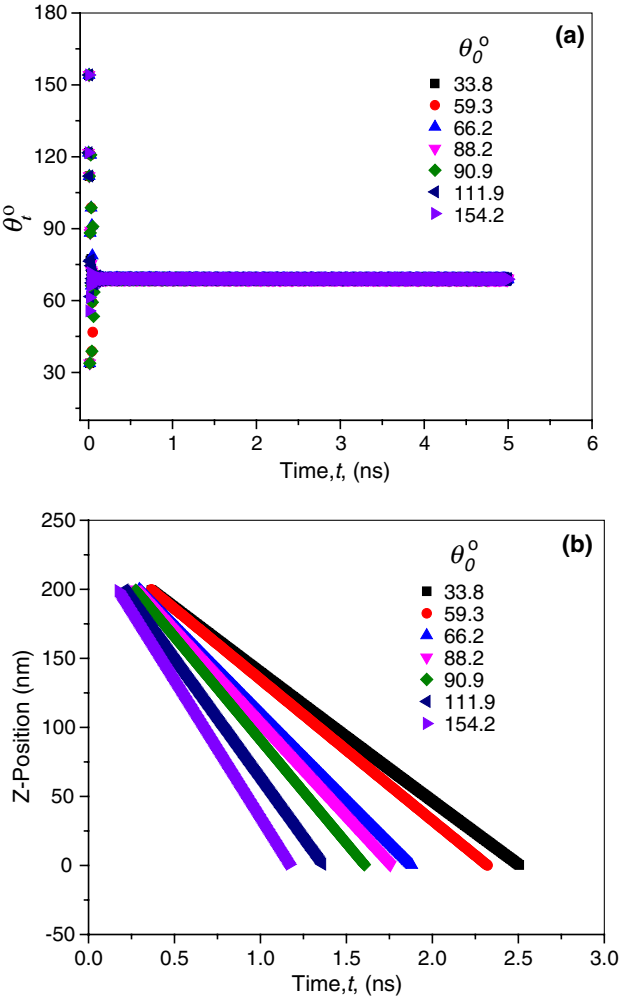

FIG. 3 (color online). Effect of the initial inclination angle upon application of the electrical field ($E = 0.02$ V/Å), θ_0 ($= \theta_{t=t_0}$), on the (a) history of θ_t and (b) axial position transport history of $H_2O@C_{60}$.

motion of $H_2O@C_{60}$, in addition to the translational motion (which is coordinated with the C_{60} cage), the encapsulated H_2O molecule also rotates around the axis of the electrical field, resulting in a circular trajectory in the projection plane perpendicular to the electrical direction (see Supplemental Material [15]).

The transport rate is investigated next. Figure 3(b) shows the effect of θ_0 on the transport trajectory of $H_2O@C_{60}$ along the z direction. Although the steady-state θ_{ts} is independent of θ_0, here the steady-state transport rate v_{ts} changes with θ_0, and a higher θ_0 results in a smaller v_{ts}. Conceptually, the electrical work required to change the single H_2O molecule from a random θ_0 to a steady θ_{ts} is $pE|\theta_0 - \theta_{ts}|\sin\theta_0$, where p is the dipole moment of the H_2O molecule ($\sim 6.2 \times 10^{-30}$ C m for SPC/E model [24]). Thus, a higher θ_0 will need more electrical work, leading to a faster transport rate.

To understand the rotational motions of the encapsulated single H_2O inside C_{60} and the induced net translational motion of $H_2O@C_{60}$ along the direction of the electrical field, we analyze the autocorrelation functions of velocity (v-ACF) and angular velocity (ω-ACF) of the encapsulated H_2O with the electrical intensity of 0.03 V/Å for a representative system, and they are defined as $\langle v(t) \cdot v(0) \rangle$ and $\langle \omega(t) \cdot \omega(0) \rangle$, respectively. The results are plotted in Fig. 5. In Fig. 5(a), the v-ACFs of v_x and v_y have similar characteristics with a superposition of a high-frequency mode and a low-frequency mode that decays much faster. The v_z has a different frequency of oscillation than the v_x and v_y. Besides, it will not approach zero due to the presence of an external electrical field in the z direction. More importantly, compared with the v_x and v_y, the v_z is closest to the v-ACF of $H_2O@C_{60}$, indicating its greatest contribution to the translational motion of $H_2O@C_{60}$ along the z direction motion. Similar results are also obtained in the ω-ACF [Fig. 5(b)]. The quick decay in both ω_x and ω_y demonstrates that librations in x and y directions decrease, and ω_z will approach zero eventually, indicating a uniform rotation around the electrical field axis (this also agrees well with Fig. S6 [15]). The quick decay in both ω_x and ω_y demonstrates that the librations around x and y directions

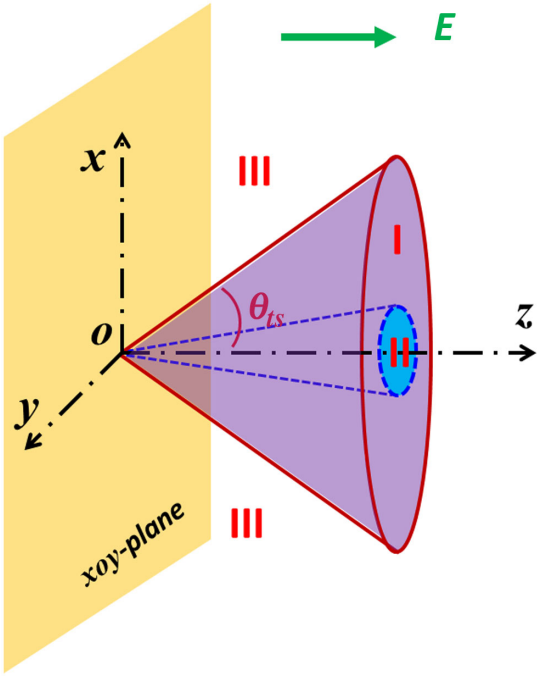

FIG. 4 (color online). Transport map of $H_2O@C_{60}$ on a CNT channel: region I ($26.7^\circ < |\theta_{ts}| < 82.6^\circ$ and $0.006\ \mathrm{V/Å} < E < 0.065\ \mathrm{V/Å}$) where the transport is opposite to the electrical field direction ($-z$); region II ($0 \le |\theta_{ts}| \le 26.7^\circ$ and $E \ge 0.065\ \mathrm{V/Å}$) where transport is along the direction of the electrical field ($+z$); region III ($0 \le E \le 0.006\ \mathrm{V/Å}$) where the transport direction is unstable.

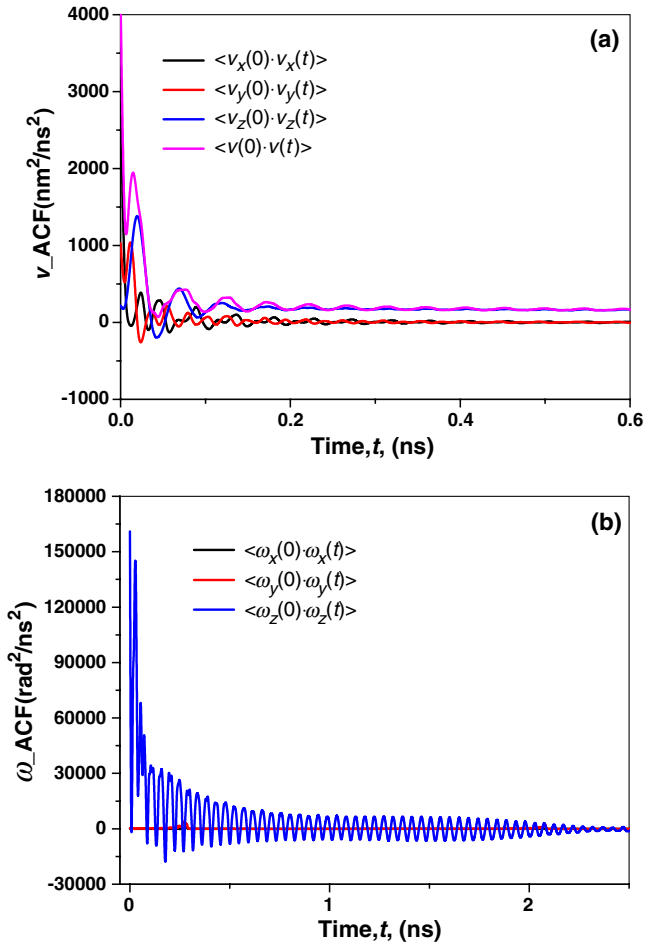

FIG. 5 (color online). Autocorrelation functions of (a) v-ACF and (b) ω-ACF of the encapsulated H_2O molecule inside C_{60} with the electrical intensity of 0.03 V/Å.

decrease, and the energy decrease of librational and rotational motions is expected to transfer to translational motion along the z direction, leading to the translational motion of $H_2O@C_{60}$ along the electrical field direction. The scarification of rotational energy around the x and y direction that gives rise to the translational motion of $H_2O@C_{60}$ along the electrical direction is further confirmed by plotting the angular-velocity cross-autocorrelation function (ω-v-ACF) for coupling between the rotational and translational motions (Fig. S7 [15]).

Since the transport rate of $H_2O@C_{60}$ depends on θ_0 [Fig. 3(a)], yet it is often desired to control the travel time of the C_{60} cagelike capsule (e.g., for targeted drug delivery [25]), based on the results in Figs. 3 and 4, we propose a strategy to manipulate both the transport direction and rate: after equilibrium of $H_2O@C_{60}$ in a channel, in spite of its random orientation angle, a preelectrical field (pE) is applied to obtain a steady transport behavior of $H_2O@C_{60}$ with a constant θ_{ts}^{pE}, and then the particle is temporarily stopped inside the transport channel (e.g., by introducing a switch to "snap" the local nanochannel size below a certain threshold [26]). Through these two steps, the orientation angle of the encapsulated H_2O molecule has been adjusted to a desired θ_{ts}^{pE}, which depends only on pE. Afterwards, a new electrical field (E) is applied while the switch is turned off (and the $H_2O@C_{60}$ is allowed to move axially again), and afterwards the $H_2O@C_{60}$ will travel at a new steady state (whose rate depends on θ_{ts}^{pE} and E, which is controllable).

In summary, we propose a new mechanism for manipulating $H_2O@C_{60}$ transport by controlling the encapsulated polar H_2O molecule through an external electrical field. Our MD simulations show that, when an external electrical field is applied properly along the axial direction of the channel, steady-state transport of $H_2O@C_{60}$ can be reached. A strategy is proposed for controlling both the transport direction and rate of $H_2O@C_{60}$ simultaneously, which may provide useful insights on targeted delivery via C_{60}-like cages.

The work is supported by National Science Foundation (CMMI-0643726), DARPA (W91CRB-11-C-0112), National Natural Science Foundation of China (11172231), Changjiang Scholar Program from Ministry of Education of China, and World Class University program through the National Research Foundation of Korea (R32-2008-000-20042-0).

*Corresponding author.
xichen@columbia.edu

[1] M. Saunders, H. A. Jimenez-Vazquez, R. J. Cross, and R. J. Poreda, Science **259**, 1428 (1993).
[2] K. Komatsu, M. Murata, and Y. Murata, Science **307**, 238 (2005).
[3] G. Liu, A. N. Khlobystov, G. Charalambidis, A. G. Coutsolelos, G. Andrew, D. Briggs, and K. Porfyrakis, J. Am. Chem. Soc. **134**, 1938 (2012).
[4] M. Saunders, H. A. Jimenez-Vazquez, R. J. Cross, S. Mroczkowski, M. L. Gross, D. E. Giblin, and R. J. Poreda, J. Am. Chem. Soc. **116**, 2193 (1994).
[5] Q. Z. T. Pankewitz, S. Liu, W. Klopper, and L. Gan, Angew. Chem., Int. Ed. **49**, 9935 (2010).
[6] F. Sebastianelli, M. Xu, Z. Bacic, R. Lawler, and N. J. Turro, J. Am. Chem. Soc. **132**, 9826 (2010).
[7] N. J. Turro, J. Y.-C. Chen, E. Sartori, M. Ruzzi, A. Marti, R. Lawler, S. Jockusch, J. Lopez-Gejo, K. Komatsu, and Y. Murata, Acc. Chem. Res. **43**, 335 (2010).
[8] K. Kurotobi and Y. Murata, Science **333**, 613 (2011).
[9] K. Koga, G. T. Gao, H. Tanaka, and X. C. Zeng, Nature (London) **412**, 802 (2001).
[10] J. Bai, J. Wang, and X. C. Zeng, Proc. Natl. Acad. Sci. U.S.A. **103**, 19 664 (2006).
[11] G. Hummer, J. G. Rasalah, and J. P. Noworyta, Nature (London) **414**, 188 (2001).
[12] S. Joseph and N. R. Aluru, Nano Lett. **8**, 452 (2008).
[13] C. Dellago, M. M. Naor, and G. Hummer, Phys. Rev. Lett. **90**, 105902 (2003).
[14] F. Mikami, K. Matsuda, H. Kataura, and Y. Maniwa, ACS Nano **3**, 1279 (2009).
[15] See Supplemental Material at http://link.aps.org/supplemental/10.1103/PhysRevLett.110.156103 for the detailed molecular dynamics force field and more MD results and analysis for motional trajectories of the encapsulated single water molecules in the electrical field. Density functional theory calculations are also performed to provide separate confirmations for MD model and results. Two typical transport directions of the $H_2O@C_{60}$ in electrical field with different intensities (0.02 V/Å and 0.1 V/Å) are given in the movies.
[16] D. Bucher, Chem. Phys. Lett. **534**, 38 (2012).
[17] H. J. C. Berendsen, J. R. Grigera, and T. P. Straatsma, J. Phys. Chem. **91**, 6269 (1987).
[18] D. Baowan, N. Thamwattana, and J. M. Hill, Phys. Rev. B **76**, 155411 (2007).
[19] M. Y. Amusia and A. S. Baltenkov, Phys. Lett. A **360**, 294 (2006).
[20] R. R. Zope, T. Baruah, M. R. Pederson, and B. I. Dunlap, Phys. Rev. B **77**, 115452 (2008).
[21] S. Plimpton, J. Comput. Phys. **117**, 1 (1995).
[22] B. Xu, Y. Qiao, Y. Li, Q. Zhou, and X. Chen, Appl. Phys. Lett. **98**, 221909 (2011).
[23] J. Li, X. Gong, H. Lu, D. Li, H. Fang, and R. Zhou, Proc. Natl. Acad. Sci. U.S.A. **104**, 3687 (2007).
[24] P. G. Kusalik and I. M. Svishchev, Science **265**, 1219 (1994).
[25] A. Montellano, T. D. Ros, A. Bianco, and M. Prato, Nanoscale **3**, 4035 (2011).
[26] R. Wan, J. Li, H. Lu, and H. Fang, J. Am. Chem. Soc. **127**, 7166 (2005).